PHYSICAL REVIEW MATERIALS **4**, 054402 (2020)

Validity of magnetotransport detection of skyrmions in epitaxial $SrRuO_3$ heterostructures

Lena Wysocki,[1,*] Lin Yang,[1] Felix Gunkel,[2] Regina Dittmann,[2] Paul H. M. van Loosdrecht,[1]
and Ionela Lindfors-Vrejoiu[1,†]
[1]*Institute of Physics II, University of Cologne, 50937 Cologne, Germany*
[2]*Peter Grünberg Institut (PGI-7), Forschungszentrum Jülich GmbH, 52428 Jülich, Germany*

(Received 19 February 2020; accepted 3 April 2020; published 4 May 2020)

A technically simple way of probing the formation of skyrmions is to measure the topological Hall resistivity that should occur in the presence of skyrmions as an additional contribution to the ordinary and anomalous Hall effect. This type of probing, lately intensively used for thin film samples, relies on the assumption that the topological Hall effect contribution can be extracted unambiguously from the measured total Hall resistivity. Ultrathin films and heterostructures of the 4*d* ferromagnet $SrRuO_3$ have stirred up a lot of attention after the observation of anomalies in the Hall resistivity, which resembled a topological Hall effect contribution. These anomalies, first reported for bilayers in which the $SrRuO_3$ was interfaced with the strong spin-orbit coupled oxide $SrIrO_3$, were attributed to the formation of tiny Néel-type skyrmions. Here we present the investigation of heterostructures with two magnetically decoupled and electrically parallel connected $SrRuO_3$ layers. The two $SrRuO_3$ layers deliberately have different thicknesses, which affects the coercive field and ferromagnetic transition temperature of the two layers, and the magnitude and temperature dependence of their anomalous Hall constants. The $SrRuO_3$ layers were separated by ultrathin layers of either the strong spin-orbit coupling oxide $SrIrO_3$ or of the large band-gap insulator $SrZrO_3$. Our magnetic and magnetotransport studies confirm the additivity of the anomalous Hall transverse voltages for the parallel conducting channels originating from the two ferromagnetic $SrRuO_3$ layers as well as the possibility to tune the global anomalous Hall resistivity by magnetic field, temperature, or structural modifications at the epitaxial all-oxide interfaces. The Hall voltage loops of these two-layer heterostructures demonstrate the possibility to generate humplike structures in the Hall voltage loops of $SrRuO_3$ heterostructures without the formation of skyrmions and emphasize that the detection of skyrmions only by Hall measurements can be misleading.

DOI: 10.1103/PhysRevMaterials.4.054402

I. INTRODUCTION

Topologically protected magnetic whirls, known as magnetic skyrmions, and the possibility of generating them in all-oxide epitaxial heterostructures are very exciting because of the prospect of controlling these robust and possibly tiny magnetic objects by electric field effects. The search for oxide heterostructures that may support the formation of skyrmions is just in its infancy, with the first papers published in 2016, related to $SrRuO_3$ heterostructures [1]. Since then epitaxial heterostructures of the 4*d* $SrRuO_3$ ferromagnet have been studied intensively, sparked by the proposal that Néel skyrmions as small as 10 nm can form in $SrRuO_3/SrIrO_3$ bilayers if the ruthenate layers are at most 6 monolayers thick [1,2]. The ultrasmall Néel skyrmions were expected to result primarily from the large interfacial Dzyaloshinskii-Moriya interaction (DMI), stemming from the breaking of the inversion symmetry at the epitaxial interface together with the large spin-orbit coupling (SOC) in $SrIrO_3$. Moreover, electric field control of skyrmions in $SrRuO_3/SrIrO_3$ heterostructures was proposed in a follow-up paper of the Kawasaki group [3]. However, a major challenge of developing oxide heterostructures to generate 10-nm large skyrmions or smaller is that there are limited experimental possibilities to image magnetic domains and to probe the real-space magnetic texture of magnetic domains with noncollinear order. Magnetic force microscopy (MFM) has limited spatial resolution (typically about 20 nm) and does not probe in-plane magnetization [1,2,4], and Lorentz transmission electron microscopy (TEM) or electron holography are challenging in view of the special TEM specimen preparation [5]. Heterostructures with $SrRuO_3$ thin layers are in particular problematic, because $SrRuO_3$ layers are sensitive to ion/electron beam induced damage during the TEM specimen processing and imaging. Therefore, alternative or complementary methods to these imaging techniques are highly needed. One way of probing the formation of skyrmions used intensively, in particular for thin film samples for which other means of investigation do not work (e.g., neutron scattering), is by measuring Hall voltage loops. This type of probing relies on the assumption that the topological Hall effect should occur in the presence of skyrmions generating a contribution appearing in addition to the anomalous Hall effect (AHE) and the ordinary Hall effect (OHE) [6]. While the ordinary Hall resistivity scales linearly with the perpendicular component of the external magnetic field, the anomalous Hall resistivity of a homogeneous ferromagnet is assumed to be proportional to the out-of-plane component of the sample magnetization [6]. For example, the formation of skyrmions in $SrRuO_3/SrIrO_3$

---

[*] Corresponding author: wysocki@ph2.uni-koeln.de

[†] Corresponding author: vrejoiu@ph2.uni-koeln.de

bilayers was inferred primarily from the observation of peculiar features (humplike) in the Hall resistivity loops when compared with the magnetization hysteresis loops [1]. The occurrence of such anomalies, resembling a topological Hall effect (THE), sometimes corroborated by MFM investigations of the magnetic domains upon running a magnetization hysteresis loop, were taken as sufficient proof for the formation of skyrmions [1–3,7]. THE-like features in the Hall resistivity loops were also observed in ultrathin bare $SrRuO_3$ films [8], for instance when the films were deliberately grown in low oxygen pressure conditions [9] or protonated after the growth [10]. Recently, alternative explanations for the anomalies of the Hall resistivity loops have been proposed, questioning the origin of the humplike features as stemming from the formation of skyrmions [11,12]. Due to the observed dominance of the intrinsic contribution to the anomalous Hall effect in bare $SrRuO_3$ films and its associated dependence on the band structure [12–14], the anomalous Hall effect was found to be sensitive to variations of the film thickness [15], the crystal structure [16], off-stoichiometry [11], and the interfacial environment [12]. It was argued that inhomogeneities within the $SrRuO_3$ films were responsible for multiple conduction channels contributing to the anomalous Hall effect [14,17–19]. Imaging the magnetic domains of $SrRuO_3/SrIrO_3$ heterostructures by magnetic force microscopy yielded also contradictory conclusions, either in favor of skyrmions [1,2] or against the formation of skyrmions [4].

Here, we demonstrate that it is possible to generate humplike structures in the Hall voltage loops of $SrRuO_3$ films without the formation of skyrmions. We aim to emphasize that solely Hall voltage measurements can be misleading and are not sufficient for the proof of skyrmion formation. For this purpose, we study the Hall voltage loops of an epitaxial heterostructure with two distinct ferromagnetic $SrRuO_3$ layers with perpendicular magnetic anisotropy (PMA), which are magnetically decoupled, but electrically connected in parallel. Hence two magnetotransport channels were generated deliberately. $SrRuO_3$ has a complex temperature dependence of the AHE resistivity, with a change of sign from negative at low temperatures to positive close to the Curie temperature (160 K) for bulk single crystals [13]. Recently it was found that for ultrathin films (thinner than 10 monolayers) the value of the magnetization controls the sign of the AHE resistivity and the change of sign occurs when the magnetic moment is about 0.5 μ_B/Ru, which is about one third of the low-temperature magnetic moment for bulk strontium ruthenate [20]. The heterostructures have two metallic ferromagnetic $SrRuO_3$ layers of two significantly different thicknesses to create sizably different magnitudes of the coercive field, of the magnetization and of the AHE constant of the two layers and also in the temperature at which the AHE constant changes sign. Additionally, only the thinner top $SrRuO_3$ layer is in a thickness range where interfacial Dzyaloshinskii-Moriya interaction may be strong enough to result in the formation of skyrmions [1]. The two $SrRuO_3$ layers are separated by nonmagnetic and insulating layers of either $SrIrO_3$ or $SrZrO_3$. These spacers were chosen having in mind the previous proposals that large DMI can emerge at the $SrRuO_3/SrIrO_3$ interface [1]. The influence of the strong SOC $SrIrO_3$ at the $SrRuO_3/SrIrO_3$ interfaces was addressed by its substitution with the band-gap insulator $SrZrO_3$, for which the strength of a possibile interfacial DMI is expected to be negligibly small. Our heterostructures resemble what was dubbed an extraordinary Hall balance, a device made of a heterostructure of two ferromagnetic layers with PMA separated by an insulating layer, designed in a previous study by Zhang *et al.* [21], which is promising for application in logic and memory elements. More important for our work, however, is that the study of the anomalous Hall voltage loops of our two-layer heterostructures brings insight into the origin of the humplike features attributed to the formation of skyrmions in several previous reports [1,3,7,9].

II. SAMPLE DESIGN AND EXPERIMENTAL METHODS

The heterostructures illustrated schematically in Fig. 1(a) are grown by pulsed-laser deposition on $SrTiO_3(100)$ substrates and have two $SrRuO_3$ layers of different thicknesses that are separated by ultrathin insulating, nonmagnetic spacers of $SrIrO_3$ (sample RIR2) or $SrZrO_3$ (sample RZR2). The layer thickness was controlled by *in situ* reflection high-energy electron diffraction (RHEED) operating in high oxygen pressure. The $SrIrO_3$ grew in a layer-by-layer mode enabling the determination of spacer and capping layer thickness during the growth [see Fig. S1(a) in Ref. [22]]. By atomic force microscopy (AFM) scanning, the heterostructure surface was found to be smooth and preserved the stepped terrace structure of the $SrTiO_3$ substrate [see Fig. S1 in Ref. [22]]. Superconducting quantum interference device (SQUID) magnetometry was performed with a commercially available SQUID magnetometer (MPMS-XL, Quantum Design Inc.). In order to extract the magnetic response of the ferromagnetic $SrRuO_3$ layers, the linear contribution of the diamagnetic $SrTiO_3$ substrate was subtracted by linear fitting in the high magnetic field range. Furthermore, the nonlinear magnetic moment measured above the Curie temperature of the $SrRuO_3$ films was subtracted to correct for additional background signal.

Hall effect measurements were carried out in the four-point van der Pauw geometry with permutating contacts for antisymmetrization. Hall voltage loops were measured with a homemade setup enabling the simultaneous measurement of transverse Hall voltage and magneto-optical Kerr effect (MOKE). The polar MOKE studies were performed with the magnetic field applied perpendicular to the thin film surface utilizing incoherent light. The wavelength was chosen individually for each sample to reduce optical artifacts such as interference effects that can be present in epitaxial multilayers. Incoherent light of 540 nm wavelength was used for the MOKE investigations of sample RIR2, and for sample RZR2 light with 590 nm wavelength. For the main heterostructure under study, sketched in Fig. 1(a) and named RIR2, the thickness of the bottom $SrRuO_3$ layer, about 18 monolayers (MLs), was chosen to stay above the limit to achieve orthorhombic structure at room temperature, but preserve coherent structure with no strain relaxation [23]. The second $SrRuO_3$ layer is only 6 MLs thick and thus has much larger coercive field and lower Curie temperature, but still has robust ferromagnetic order with Curie temperature above 100 K [15,24]. Such a two-$SrRuO_3$-layer heterostructure enabled us to study the magnetic interlayer coupling in a previous study [25]. We

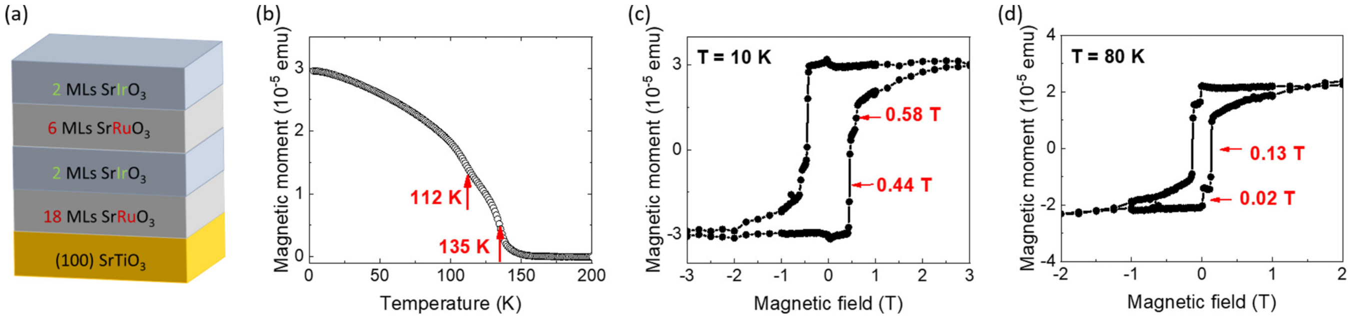

FIG. 1. (a) Scheme of the main investigated heterostructure RIR2: 18-ML-thick bottom $SrRuO_3$ layer, with spacer of 2-ML-thick $SrIrO_3$, and with 6-ML-thick top $SrRuO_3$ layer capped with 2-ML-thick $SrIrO_3$, grown on $SrTiO_3(100)$ substrate. SQUID magnetometry of the sample: (b) Temperature dependence of the magnetic moment during warming up in the presence of 0.1 T, after field cooling in 0.1 T; saturated magnetic hysteresis loops at 10 K (c) and 80 K (d). The magnetization reversal field values for the two $SrRuO_3$ layers are given on the loops in red.

found that the ruthenate layers are basically decoupled with very weak ferromagnetic coupling down to 10 K, when the spacer was a $SrIrO_3/SrZrO_3$ bilayer as thin as 2 MLs. To test that the two magnetic layers of the heterostructure RIR2 are decoupled, magnetization measurements were performed. As depicted in Fig. 1(b), two ferromagnetic transitions were observed in the field-cooled measurement of the magnetization as a function of temperature. The lower one at temperature $T_C = 112\,K$ can be attributed to the transition of the 6-ML $SrRuO_3$ layer, and the one at $T_C = 135\,K$ must be due to the 18-ML $SrRuO_3$ layer. The expected difference in coercive fields of the two $SrRuO_3$ layers was observed in the magnetization hysteresis loops, shown in Fig. 1. The hysteresis loops exhibit double-step-like magnetization reversal behavior. At low temperatures such as 10 K [Fig. 1(c)], the thick $SrRuO_3$ layer reverses magnetization around 0.44 T and the thin layer around 0.58 T, but at high temperatures (above 50 K) the thick layer has a larger coercive field than the thin layer [see Fig. 1(d) for the loop measured at 80 K]. This is related to the different dependence on temperature for the domain nucleation and coercive fields of the two layers, as we found previously [25]. The two-step magnetization reversal behavior strongly indicates that the magnetic coupling of the two ruthenate layers of the heterostructure under study is fairly weak (as will be demonstrated from the minor loop measurements discussed later and also in [25]) and thus here we consider the layers to be magnetically decoupled.

III. RESULTS

A. Two-layer heterostructure with $SrIrO_3$ spacer (RIR2)

In the model of parallel connected and magnetically decoupled ferromagnetic (FM) layers, the Hall voltages generated by the layers sum up [21,26,27]. The total Hall voltage V_{xy} loops of the heterostructure RIR2, measured with the magnetic field applied perpendicular to the sample surface, are presented in Fig. 2. In our heterostructure composed of two magnetically decoupled FM layers with PMA, an unconventional shape of the Hall voltage is observed in a broad temperature range. The loops measured below 110 K, when both $SrRuO_3$ layers become ferromagnetic, exhibit humplike features similar to those previously observed in $SrRuO_3/SrIrO_3$ bilayers, which have been related either to skyrmions [1,2] or to the existence of multiple conduction channels [12]. The humplike features of the loops have a rather flat plateaulike shape between 80 and 100 K. The features are becoming apparently more peaklike for temperatures below 80 K. At

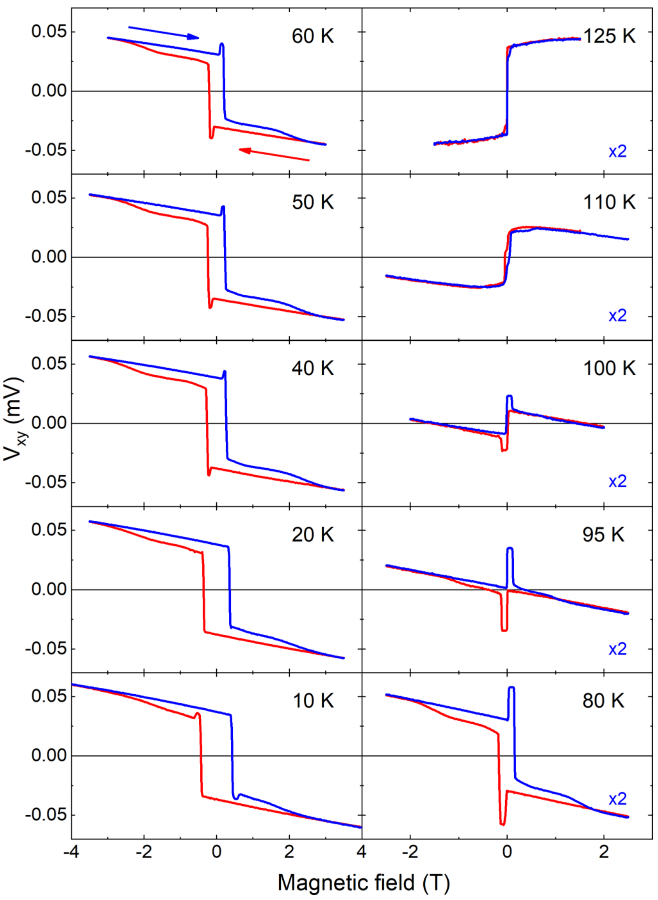

FIG. 2. Hysteresis loops of the magnetic field dependence of the total Hall voltage V_{xy} of the RIR2 heterostructure described in Fig. 1, at selected temperatures, capturing the global change of sign of the anomalous Hall effect above 95 K. The arrows in the top left panel (60 K loop) indicate the direction in which the magnetic field was swept while we acquired the full loops.

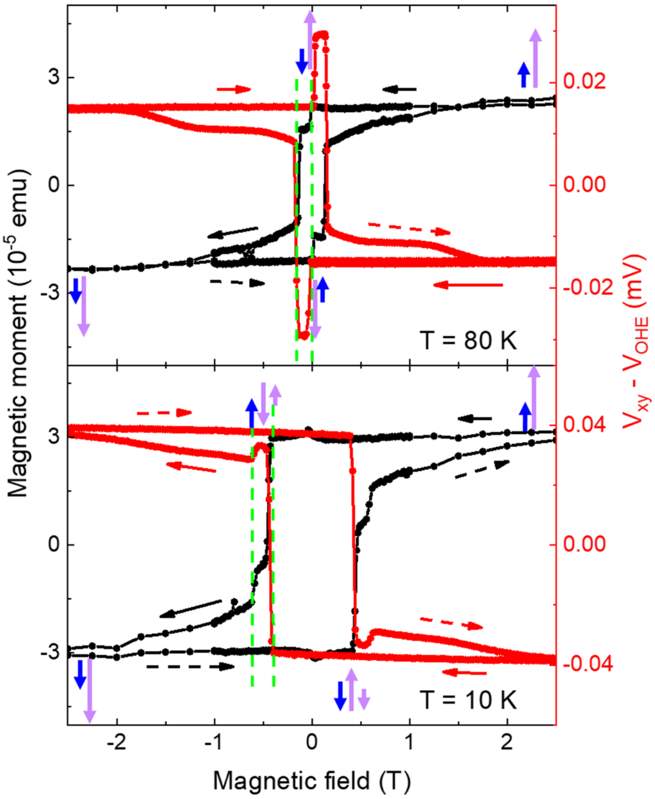

FIG. 3. Magnetic moment (black) and Hall voltage loops (after subtraction of the ordinary Hall effect contribution, shown in red) of the RIR2 heterostructure between saturated magnetization states of opposite polarities, at 10 K (lower panel) and at 80 K (upper panel). The vertical arrows indicate the orientation of the out-of-plane magnetization of the thin (blue arrows) and thick $SrRuO_3$ layers (purple arrows) when the magnetic field is swept from +3 to −3 T and then reversed. The horizontal and tilted arrows guide the reader along the magnetic moment (black) and Hall voltage (red) loops, respectively. The magnetic moment loops were measured by the SQUID magnetometer.

10 K, the Hall voltage exhibits a somewhat more surprising behavior with dips in the loops immediately after the thicker layer reverses its magnetization. We will analyze in more detail this peculiar behavior of the 10-K loop below.

We note here that the ordinary Hall voltage contribution was subtracted from the total Hall voltage for the Hall loops shown subsequently throughout the paper. The magnetic field range in which the anomalies in the Hall loops occur coincides with the field range in which the magnetization of one of the two ferromagnetic layers (the one with lower coercivity at that particular temperature) reverses its direction following the orientation of the applied field (data summarized in Fig. 3). The extent of this magnetic field range is marked by the dashed green lines in Fig. 3. At 80 K, at which the thin top $SrRuO_3$ layer has lower coercive field, the humplike anomalies reach their maximum in a magnetic field range where the magnetizations of both $SrRuO_3$ layers are saturated, but oriented in opposite directions. Therefore, these anomalies cannot be correlated with magnetic domains formed in the process of the magnetization reversal of the thin top $SrRuO_3$ layer between saturated states. This is an important observation that makes the formation of skyrmions in the 6-ML-thick $SrRuO_3$ layer, while running the hysteresis loop of the magnetization reversal, unlikely. Under the assumption that the THE contribution due to the formation of skyrmions is ignored, the subtraction of the ordinary Hall voltage V_{OHE} from the total Hall voltage V_{xy} yields the total anomalous Hall voltage V_{AHE} of the heterostructure. The well-matching coincidence of the field range strongly indicates that the humplike features of the Hall loops originate from the existence of magnetic subsystems with distinct magnetotransport characteristics, i.e., different sign and magnitude of the individual AHE constants. In the case of two decoupled magnetic subsystems contributing to the anomalous Hall voltage, the empirical description that assumes the direct proportionality of the AHE voltage V_{AHE} and the out-of-plane component of the total sample magnetization $M_\perp$ [28,29], needs to be tested. Most likely each subsystem has a different anomalous Hall constant R_{AH}, with possibly different sign and magnitude, and also different temperature dependences.

The measured AHE voltage is given by the sum of all subsystem contributions if the systems are coupled electrically. The perpendicular component of the total magnetic moment of the heterostructure is the sum of the contributions of the two magnetic subsystems, where the one with smaller magnetic moment can be related to the 6-ML $SrRuO_3$ layer. At 10 K, the thicker layer has a lower switching field, whereas the thinner layer switches at smaller magnetic field at elevated temperatures, such as at 80 K (see Fig. 3, and more details in [25]).

To separate the AHE contribution of the two ferromagnetic layers to the total AHE voltage loops, minor loop measurements were performed. We show in Fig. 4 the measurements of minor loops of the Hall voltage, corrected for the ordinary Hall voltage, and of the magnetic moment at 10 and 50 K. The RIR2 heterostructure was saturated in a positive magnetic field of 3 T, then the field was decreased to zero and its polarity was reversed and its magnitude increased in order to switch the magnetization of the layer with lower switching field. We returned the minor loop for a magnetic field value at the middle of the first plateau, which we assumed to correspond to the range where the magnetically harder layer was still saturated and the softer layer had already reversed its magnetization, and sweeped the field back to positive values and up to 3 T. The minor loop investigations yielded information concerning the magnetic hysteresis behavior of the softer $SrRuO_3$ layer and thus of the corresponding changes of the anomalous Hall voltage. Additionally the analysis of the shifts of the minor loops with respect to the full loops, which turned out to be tiny, enabled the assessment of the magnetic interlayer coupling, concluding that the two $SrRuO_3$ layers are basically magnetically decoupled [25].

The minor loop measured at 50 K [Fig. 4(b)] corresponds to the complete magnetization reversal of the top 6-ML $SrRuO_3$ layer. The Hall voltage minor loop, having the same sign as the magnetic moment minor loop (AHE scale was inverted for better comparison), illustrates that the AHE constant of the top 6-ML $SrRuO_3$ layer is positive at 50 K, while the AHE constant of the thick bottom $SrRuO_3$ layer must be negative and makes the dominant contribution to the total AHE loop. At 10 K, the switching field of the thicker layer is

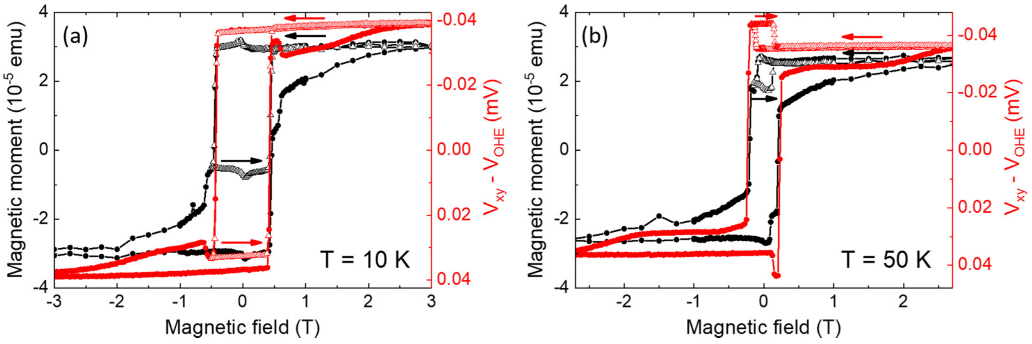

FIG. 4. Comparison of full loops (solid symbols) and minor loops (open symbols) of the Hall voltage after the subtraction of the ordinary Hall contribution (red, scale inverted) and the magnetic moment (black) at 10 K (a) and 50 K (b) for the RIR2 heterostructure. The sign of the Hall voltage values is inverted for the sake of direct comparison to the magnetic moment loop.

smaller and thus the minor loops relate to the magnetization reversal of the bottom $SrRuO_3$ layer. It also shows that the AHE constant of the bottom layer is negative down to 10 K, as expected for relatively thick $SrRuO_3$ films [30]. In the Supplemental Material (see Fig. S4 in Ref. [22]) we show also Hall loop measurements of a trilayer with a 6-ML-thick $SrRuO_3$ film sandwiched between two $SrIrO_3$ layers (2 MLs thick). For the $SrRuO_3$ in the trilayer, the AHE constant changes sign from negative to positive as the temperature increases a little above 80 K, and has a Curie temperature of about 126 K. No humplike anomalies were observed for the Hall loops in the entire ferromagnetic range down to 10 K. The behavior of the AHE of the 6-ML-thick $SrRuO_3$ in the trilayer sample is different from what we inferred for the top 6-ML-thick $SrRuO_3$ layer of sample RIR2: this observation stresses how dramatically the properties of $SrRuO_3$ depend on all the sample details.

Both the temperature range in which the humplike anomalies of the Hall loops appear and their shape can be explained with a simple model: If the occurrence of a topological Hall effect due to skyrmions is not taken into account, the difference of the total Hall voltage and the ordinary Hall voltage ($V_{xy} - V_{OHE}$) will be the total anomalous Hall voltage of the heterostructure V_{AHE}. Assuming a two-channel model (see Ref. [22] for details), we can decompose the magnetic moment and the anomalous Hall voltage loops in two independent contributions [see Fig. 5(a)]. This could be done for loops measured at any temperature in the ferromagnetic range of both the thin and thick $SrRuO_3$ layers of sample RIR2. Hence, we can derive the temperature dependence of the AHE voltages and of the switching fields of the two $SrRuO_3$ layers and get a qualitative understanding of the humplike anomalies observed in the AHE voltage loops. The anomalous Hall voltage generated in the two ferromagnetic $SrRuO_3$ layers was calculated from the minor loop measurements (see Fig. 4 and details in Ref. [22]). At a certain temperature, the AHE voltage of the magnetically softer layer is given by the half of the AHE voltage change of the minor loop, if we disregard the tail in the hysteresis loops (occurring at high fields); the anomalous Hall voltage of the magnetically harder layer is then calculated by subtracting the minor loop contribution from the total AHE voltage in saturation. We found that the 18-ML $SrRuO_3$ layer shows a nonlinear temperature dependence of the AHE voltage, including the change of sign from negative to positive values at 110 K, close to the ferromagnetic phase transition, as is common for the anomalous Hall effect of orthorhombic bare $SrRuO_3$ films of similar thickness [15,30–33] and single crystals [13]. In contrast, from our evaluation the anomalous Hall voltage of the 6-ML $SrRuO_3$ layer, which has two interfaces with the strong SOC $SrIrO_3$,

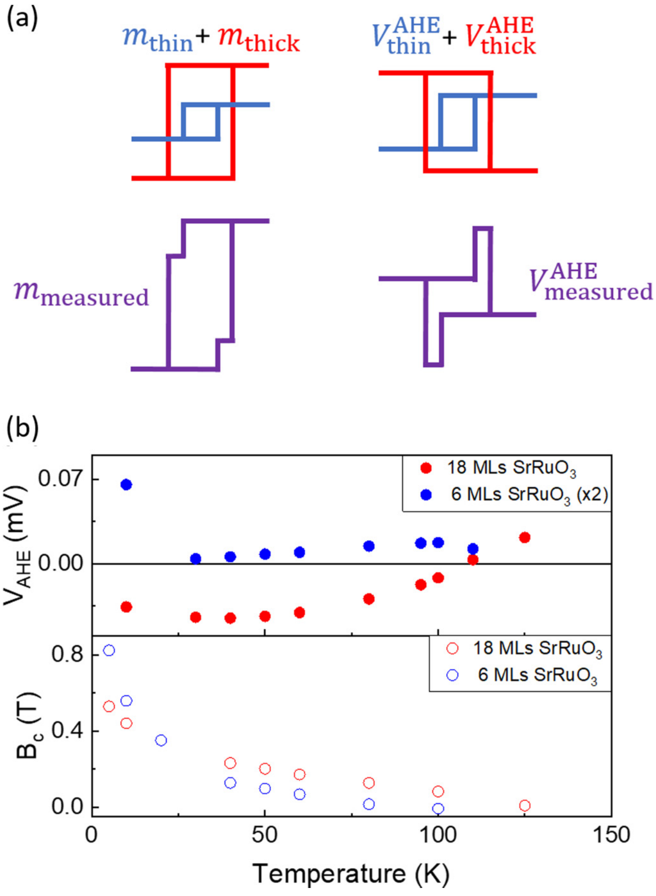

FIG. 5. (a) Scheme of the magnetization and the anomalous Hall voltage loops for a two-channel model, which was used to determine the AHE voltages generated in the two individual $SrRuO_3$ layers (solid circles) and the switching fields (open circles) of the 18-ML $SrRuO_3$ layer (red) and of the 6-ML $SrRuO_3$ layer (blue) plotted in (b).

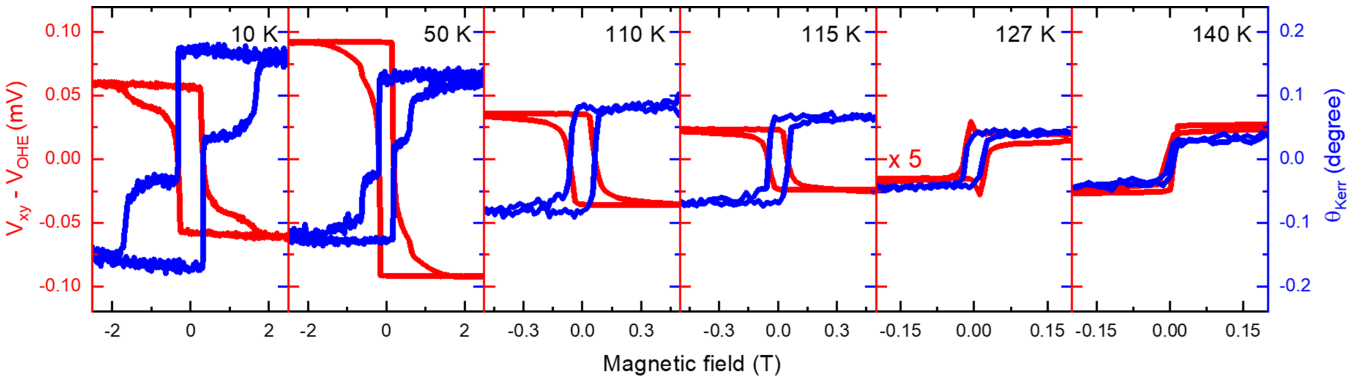

FIG. 6. Hall voltage hysteresis loops after subtraction of the ordinary Hall contribution (red) and Kerr rotation angle loops (blue) as a function of temperature for the heterostructure with $SrZrO_3$ spacer and capping layer (sample RZR2), capturing the global change of sign of the AHE from negative to positive above 127 K. The Hall and MOKE loops were measured simultaneously under the same conditions. Note that the Hall voltage values at 127 K are multiplied by 5.

is positive down to 10 K (see Ref. [22] for details). This behavior is unconventional for bare $SrRuO_3$ thin films, but was observed in symmetric $SrIrO_3/SrRuO_3/SrIrO_3$ trilayers before [12]. From our analysis based on the simple additivity of the two independent AHE channels, we conclude that, in order to account for humplike anomalies, the switching fields need to be different and the sign of the AHE voltage, which scales linearly with the AHE constant, needs to be opposite for the two $SrRuO_3$ layers. These conditions are readily fulfilled between 40 and 100 K, in agreement with the experimental data summarized in Fig. 2. The difference in shape between the loops at 10 K and above 40 K is related to the fact that somewhere below 40 K the thin top $SrRuO_3$ layer becomes the magnetically hard layer, while its coercive field is sizably larger than the coercive field of the bottom thick layer for temperatures above 40 K (see also the MOKE measurements of the RIR2 sample shown in Sec. 2 in Ref. [22]). We discussed the temperature dependence of the coercive fields of the two $SrRuO_3$ layers in detail in our previous publication and in its Supplemental Material [25]. For temperatures somewhat lower than 40 K, the 18-ML $SrRuO_3$ has a lower switching field and starts reversing its magnetization before the 6-ML $SrRuO_3$ layer, but it does not complete its reversal before the thin layer starts switching as well. Part of the thick film is still unswitched and results in the tail of the hysteresis loops and it is most likely related to strongly pinned domains in the 18-ML $SrRuO_3$ layer. This additional tail present in the magnetic hysteresis loops was observed previously for thick $SrRuO_3$ films [30] and for similar heterostructures, $SrRuO_3/SrIrO_3/SrZrO_3$ trilayers [25]. Recently it was proposed that the pinning of the magnetic domains originates from disorder of the crystallographic orientation of the films grown on $SrTiO_3$ substrates with low vicinal angle [34]. Zahradnic *et al.* showed that the size of the nucleation magnetic domains is larger and the pinning is less strong if the $SrRuO_3$ epitaxial films are grown on highly vicinal substrates (1° instead of 0.1° miscut angle). Our simple model analysis assumes that magnetization saturation is reached sharply at the value of the larger switching field ([see Fig. 5(a)] and thus it does not account for the contribution of the strongly pinned domains, which generate the tail present at magnetic fields larger than the switching fields of the two layers. In Fig. 5(b) we plotted also the temperature dependence of the switching fields of each layer determined from the minimum of the derivative of the magnetic moment. Similar humplike features of the AHE loops and double-step-like magnetic switching behavior were observed in our two-layer asymmetric heterostructure with hybrid insulating spacer consisting of 2 MLs $SrIrO_3$/2 MLs $SrZrO_3$ that were studied in [25]. The top $SrRuO_3$ has now asymmetric interfaces and for such a structure a net interfacial DMI could yield. As shown in Sec. 3 in Ref. [22], the humplike anomalies are present in a finite temperature range between 100 and 110 K, which is an indication that the AHE constant of the 6-ML $SrRuO_3$ layer of this heterostructure reverses its sign to positive values close to 100 K.

B. Two-layer heterostructure with $SrZrO_3$ spacer (RZR2)

In order to address the influence of the type of oxide interfaces on the global magnetotransport properties of the heterostructure, we substituted the oxide spacer with the large band-gap insulator $SrZrO_3$. We made the sample RZR2 with 2-ML-thick $SrZrO_3$ spacer and capping layer, which preserved the heterostructure design from Fig. 1(a). The Hall voltage, corrected for the ordinary Hall contribution, and the Kerr rotation angle loops of the heterostructure RZR2 are shown in Fig. 6. The magneto-optical Kerr rotation angle (θ_{Kerr}), which is proportional to the out-of-plane magnetization of the ferromagnetic layers, shows clear double-step switching below 50 K, because the two distinct $SrRuO_3$ layers possess different coercive fields and are magnetically decoupled because of the insulating $SrZrO_3$ spacer [25]. We note that the Hall voltage values at 127 K are multiplied by 5, as the signal is tiny, as both AHE constants are almost zero at this temperature. In contrast to the heterostructure having $SrIrO_3$ as spacer, sharp humplike anomalies are present in the Hall voltage only in a narrow temperature range close to the AHE sign change temperature between 127 and 129 K. The overall behavior of the Hall voltage loops summarized in Fig. 6 is consistent with the AHE constants of both $SrRuO_3$ layers being negative below 122 K and the top thin layer changes first sign to positive in the range

122–125 K, while the bottom thick layer changes sign to positive around 130 K, as it has larger Curie temperature (around 140 K).

We stress that in contrast to the top thin layer of RIR2 heterostructure, whose AHE constant is positive in the whole range from 10 K to Curie temperature, for the top thin layer of the RZR2 heterostructure the AHE constant behaves conventionally, showing the change of sign from negative to positive at a temperature close to the Curie temperature [13,30]. This striking difference in the behavior of the AHE constant demonstrates the importance of electronic property modifications of the 6-ML-thick $SrRuO_3$ layer at the interface with $SrIrO_3$. Most likely significant electronic band structure modifications occur as a result of interfacing $SrRuO_3$ with $SrIrO_3$ and affect the AHE conductivity, as addressed in a recent report of the results of angle-resolved photoemission spectroscopy study of ultrathin $SrRuO_3$ films [20]. Sohn *et al.* showed that the sign of the AHE can be controlled by changing the $SrRuO_3$ film thickness, magnetization, and chemical potential, and their study provided strong direct evidence for relating the topological band structure of two-dimensional spin-polarized conduction bands and the corresponding AHE conductivity. Concerning the impact of the interfacial details on the properties of the bottom 18-ML $SrRuO_3$ layers, we point out that the temperature at which the AHE sign change occurs depends strongly on the type of spacer (whether $SrIrO_3$ or $SrZrO_3$). For the heterostructure RZR2 with $SrZrO_3$ spacer, the temperature of the AHE sign change is close to 130 K, but it is around 110 K for the RIR2 heterostructure with $SrIrO_3$ spacer. Such tailoring of the magnetotransport properties of both $SrRuO_3$ layers by changing the interfacial environment stresses the importance of the interfaces on the global properties of $SrRuO_3$. Our recent work on asymmetric multilayers of $SrZrO_3/SrRuO_3/SrHfO_3$ and $SrZrO_3/SrRuO_3/SrIrO_3$ demonstrated also how important the impact of the $SrRuO_3/SrIrO_3$ interface is for the overall magnetotransport properties [35].

IV. SUMMARY

The possibility of examining the formation of skyrmions by magnetotransport measurements is very attractive as Hall resistivity investigations are rather easy to perform in any modern laboratory. Recently the great importance of the topological Hall effect for the electrical detection of single magnetic skyrmions was demonstrated for metallic multilayers, where the formation of skyrmions had been previously proved by complementary investigations as well [36]. However, lately there have been many reports in which the formation of skyrmions in $SrRuO_3$-based heterostructures was deduced primarily based on particular anomalies of Hall resistivity loops that were attributed to topological Hall effect contributions [1,3,7,9]. Alternative explanations for the anomalies of the Hall resistivity loops have been nonetheless proposed, questioning the origin of the humplike features as stemming from skyrmions, but rather from inhomogeneity of the AHE conductivity [11,12,18]. Therefore, we dedicated this magnetotransport study to $SrRuO_3$-based heterostructures, with intentional heterogeneity and with two independent conduction channels. One of the $SrRuO_3$ layers of the heterostructures under study is in a thickness range for which it was predicted that a strong DMI can exist at its interface with $SrIrO_3$ [1], and consequently skyrmion formation would be possible. However, our study proves that the anomalous Hall voltage is additive for electrically connected and magnetically decoupled $SrRuO_3$ layers separated by ultrathin $SrIrO_3$. The humplike anomalies of the AHE hysteresis loops are well described by a model of two independent magnetic subsystems exhibiting distinct coercive field magnitudes and signs of the individual anomalous Hall constants. We also point out that the AHE conductivity of $SrRuO_3$ is highly sensitive to manifold influences, via electronic band structure modifications, in our case resulting from interfacing with oxides with different electronic properties ($SrIrO_3$ vs $SrZrO_3$). The AHE of $SrRuO_3$ thin films was demonstrated to exhibit sign reversal depending on film thickness, temperature, magnetization, and chemical potential, due to the sensitivity of the symmetry-protected nodal structures of 2D spin-polarized bands to all these and possibly other factors [20]. We conclude that relying solely on measurements of AHE resistance loops for unambiguous detection of the formation of skyrmions during the magnetization reversal between saturated states in $SrRuO_3$ heterostructures can be misleading.

ACKNOWLEDGMENTS

We thank Rene Borowski for treating the termination of the substrates. We are grateful to Jörg Schöpf for the concept and construction of the Hall part of the MOKE setup and for helpful assistance and discussions, and to Andrea Bliesener for AFM investigations. We thank Michael Ziese for valuable advice concerning Hall and SQUID measurements. P.vL. and I.L.V. thank German Research Foundation (DFG) for funding the purchase of the PLD-RHEED system at University of Cologne, with which some of the investigated samples were grown (Project No. 407456390). The PLD-RHEED system was purchased in 2019 from Firma SURFACE systems+technology GmbH und Co. KG. I.L.V. acknowledges DFG for financial support via Projects No. 335038432 and No. 403504808, the latter under SPP 2137 Skyrmionics, and through Collaborative Research Center 1238 of DFG (Project No. 277146847).

---

[1] J. Matsuno, N. Ogawa, K. Yasuda, F. Kagawa, W. Koshibae, N. Nagaosa, Y. Tokura, and M. Kawasaki, Interface-driven topological Hall effect in $SrRuO_3$-$SrIrO_3$ bilayer, Sci. Adv. **2**, e1600304 (2016).

[2] K.-Y. Meng, A. S. Ahmed, M. Baćani, A.-O. Mandru, X. Zhao, N. Bagués, B. D. Esser, J. Flores, D. W. McComb, H. J. Hug, and F. Yang, Observation of nanoscale skyrmions in $SrIrO_3/SrRuO_3$ bilayers, ACS Nano Lett. **19**, 3169 (2019).

[3] Y. Ohuchi, J. Matsuno, N. Ogawa, Y. Kozuka, M. Uchida, Y. Tokura, and M. Kawasaki, Electric-field control of anomalous and topological Hall effects in oxide bilayer thin films, Nat. Commun. **9**, 213 (2018).

[4] G. Malsch, D. Ivaneyko, P. Milde, L. Wysocki, L. Yang, P. H. M. van Loosdrecht, I. Lindfors-Vrejoiu, and L. M. Eng, Correlating the nanoscale structural, magnetic, and magneto-transport properties in $SrRuO_3$-based perovskite thin flms: Implications for oxide skyrmion devices, ACS Appl. Nano Mater. **3**, 1182 (2020).

[5] M. Nakamura, D. Morikawa, X. Yu, F. Kagawa, T.-h. Arima, Y. Tokura, and M. Kawasaki, Emergence of topological Hall effect in half-metallic manganite thin films by tuning perpendicular magnetic anisotropy, J. Phys. Soc. Jpn. **87**, 074704 (2018).

[6] N. Nagaosa and Y. Tokura, Topological properties and dynamics of magnetic skyrmions, Nat. Nanotechnol. **8**, 899 (2013).

[7] B. Pang, L. Zhang, Y. B. Chen, J. Zhou, S. Yao, S. Zhang, and Y. Chen, Spin-glass-like behavior and topological Hall effect in $SrRuO_3/SrIrO_3$ superlattices for oxide spintronics applications, ACS Appl. Mater. Interfaces **9**, 3201 (2017).

[8] B. Sohn, B. Kim, S. Y. Park, H. Y. Choi, J. Y. Moon, T. Choi, Y. J. Choi, T. W. Noh, H. Zhou, S. H. Chang, J. H. Han, and C. Kim, Emergence of robust 2D skyrmions in $SrRuO_3$ ultrathin film without the capping layer, arXiv:1810.01615.

[9] Q. Qin, L. Liu, W. Lin, X. Shu, Q. Xie, Z. Lim, C. Li, S. He, G. M. Chow, and J. Chen, Emergence of topological Hall effect in a $SrRuO_3$ single layer, Adv. Mater. **31**, 1807008 (2019).

[10] Z. Li, S. Shen, Z. Tian, K. Hwangbo, M. Wang, Y. Wang, F. M. Bartram, L. He, Y. Lyu, Y. Dong, G. Wan, H. Li, N. Lu, J. Zang, H. Zhou, E. Arenholz, Q. He, L. Yang, W. Luo, and P. Yu, Reversible manipulation of the magnetic state in $SrRuO_3$ through electric-field controlled proton evolution, Nat. Commun. **11**, 184 (2020).

[11] D. Kan and Y. Shimakawa, Defect-induced anomalous transverse resistivity in an itinerant ferromagnetic oxide, Phys. Status Solidi B **255**, 1800175 (2018).

[12] D. J. Groenendijk, C. Autieri, T. C. van Thiel, W. Brzezicki, N. Gauquelin, P. Barone, K. H. W. van den Bos, S. van Aert, A. Filippetti, S. Picozzi, M. Cuoco, and A. D. Caviglia, Berry phase engineering at oxide interfaces, arXiv:1810.05619v1.

[13] Z. Fang, N. Nagaosa, K. S. Takahashi, A. Asamitsu, R. Mathieu, T. Ogasawara, H. Yamada, M. Kawasaki, Y. Tokura, and K. Terakura, The anomalous Hall effect and magnetic monopoles in momentum space, Science **302**, 92 (2003).

[14] L. Wu, F. Wen, Y. Fu, J. H. Wilson, X. Liu, Y. Zhang, D. M. Vasiukov, M. S. Kareev, J. H. Pixley, and J. Chakhalian, Berry phase manipulation in ultrathin $SrRuO_3$ films, arXiv:1907.07579.

[15] N. Haham, Y. Shperber, M. Schultz, N. Naftalis, E. Shimshoni, J. W. Reiner, and L. Klein, Scaling of the anomalous Hall effect in $SrRuO_3$, Phys. Rev. B **84**, 174439 (2011).

[16] F. Bern, M. Ziese, K. Dörr, A. Herklotz, and I. Vrejoiu, Hall effect of tetragonal and orthorhombic $SrRuO_3$ films, Phys. Status Solidi (RRL) **7**, 204 (2013).

[17] D. Kan, T. Moriyama, K. Kobayashi, and Y. Shimakawa, Alternative to the topological interpretation of the transverse resistivity anomalies in $SrRuO_3$, Phys. Rev. B **98**, 180408(R) (2018).

[18] D. Kan, T. Moriyama, and Y. Shimakawa, Field-sweep-rate and time dependence of transverse resistivity anomalies in ultrathin $SrRuO_3$ films, Phys. Rev. B **101**, 014448 (2020).

[19] L. Wang, Q. Feng, H. G. Lee, E. K. Ko, Q. Lu, and T. W. Noh, Controllable thickness inhomogeneity and Berry-curvature engineering of anomalous Hall effect in $SrRuO_3$ ultrathin films, Nano Lett. **20**, 2468 (2020).

[20] B. Sohn, E. Lee, W. Kyung, M. Kim, H. Ryu, J. S. Oh, D. Kim, J. K. Jung, B. Kim, M. Han, T. W. Noh, B.-J. Yang, and C. Kim, Sign-tunable anomalous Hall effect induced by symmetry-protected nodal structures in ferromagnetic perovskite oxide thin films, arXiv:1912.04757.

[21] S. L. Zhang, Y. Liu, L. J. Collins-McIntyre, T. Hesjedal, J. Y. Zhang, S. G. Wang, and G. H. Yu, Extraordinary Hall balance, Sci. Rep. **3**, 2087 (2013).

[22] See Supplemental Material at http://link.aps.org/supplemental/10.1103/PhysRevMaterials.4.054402 for additional information on the pulsed laser deposition, polar MOKE investigations of the heterostructure RIR2, polar MOKE and Hall investigations of the heterostructure RIZR2, and polar MOKE and Hall studies of a $SrIrO_3/SrRuO_3/SrIrO_3$ trilayer as reference sample.

[23] S. H. Chang, Y. J. Chang, S. Y. Jang, D. W. Jeong, C. U. Jung, Y.-J. Kim, J.-S. Chung, and T. W. Noh, Thickness-dependent structural phase transition of strained $SrRuO_3$ ultrathin films: The role of octahedral tilt, Phys. Rev. B **84**, 104101 (2011).

[24] J. Xia, W. Siemons, G. Koster, M. R. Beasley, and A. Kapitulnik, Critical thickness for itinerant ferromagnetism in ultrathin films of $SrRuO_3$, Phys. Rev. B **79**, 140407(R) (2009).

[25] L. Wysocki, R. Mirzaaghayev, M. Ziese, L. Yang, J. Schöpf, R. B. Versteeg, A. Bliesener, J. Engelmayer, A. Kovács, L. Jin, F. Gunkel, R. Dittmann, P. H. M. van Loosdrecht, and I. Lindfors-Vrejoiu, Magnetic coupling of ferromagnetic $SrRuO_3$ epitaxial layers separated by ultrathin non-magnetic $SrZrO_3/SrIrO_3$, Appl. Phys. Lett. **113**, 192402 (2018).

[26] S. L. Zhang and T. Hesjedal, The magneto-Hall difference and the planar extraordinary Hall balance, AIP Adv. **6**, 045019 (2016).

[27] A. Gerber, Interpretation of experimental evidence of the topological Hall effect, Phys. Rev. B **98**, 214440 (2018).

[28] E. M. Pugh and N. Rostoker, Hall effect in ferromagnetic materials, Rev. Mod. Phys. **25**, 151 (1953).

[29] N. Nagaosa, J. Sinova, S. Onoda, A. H. MacDonald, and N. P. Ong, Anomalous Hall effect, Rev. Mod. Phys. **82**, 1539 (2010).

[30] M. Ziese, F. Bern, P. D. Esquinazi, and I. Lindfors-Vrejoiu, Topological signatures in the Hall effect of $SrRuO_3/La_{0.7}Sr_{0.3}MnO_3$ SLs, Phys. Status Solidi B, 1900628 (2019), doi: 10.1002/pssb.201900628.

[31] M. Izumi, K. Nakazawa, Y. Bando, Y. Yoneda, and H. Terauchi, Magnetotransport of $SrRuO_3$ thin film on $SrTiO_3(001)$, J. Phys. Soc. Jpn. **66**, 3893 (1997).

[32] L. Klein, J. R. Reiner, T. H. Geballe, M. R. Beasley, and A. Kapitulnik, Extraordinary Hall effect in $SrRuO_3$, Phys. Rev. B **61**, R7842(R) (2000).

[33] M. Schultz, J. W. Reiner, and L. Klein, The extraordinary Hall effect of $SrRuO_3$ in the ultrathin limit, J. Appl. Phys. **105**, 07E906 (2009).

[34] M. Zahradník, K. Uhlířová, T. Maroutian, G. Kurij, G. Agnus, M. Veis, and P. Lecoeur, Magnetic domain wall motion in $SrRuO_3$ thin films, Mater. Des. **187**, 108390 (2020).

[35] L. Wysocki, J. Schöpf, M. Ziese, L. Yang, A. Kovács, L. Jin, R. B. Versteeg, A. Bliesener, F. Gunkel, L. Kornblum, R. Dittmann, P. H. M. van Loosdrecht, and I. Lindfors-Vrejoiu, Electronic inhomogeneity influence on the anomalous Hall resistivity loops of $SrRuO_3$ epitaxially interfaced with 5*d* perovskites, ACS Omega **5**, 5824 (2020).

[36] D. Maccariello, W. Legrand, N. Reyren, K. Garcia, K. Bouzehouane, S. Collin, V. Cros, and A. Fert, Electrical detection of single magnetic skyrmions in metallic multilayers at room temperature, Nat. Nanotechnol. **13**, 233 (2018).